Memo 3

Simulating radio light curves for supernovae in VAST

Stuart Ryder

October 11 2010

Simulating radio light curves for supernovae in VAST

Stuart Ryder, Australian Astronomical Observatory
sdr@aao.gov.au

October 11, 2010

1 Introduction

Radio studies of supernovae (SNe) can provide valuable information about the density structure of the circumstellar medium (CSM) and the late stages of stellar mass-loss (Weiler et al., 2002). Furthermore, with the realisation that some Gamma-Ray Bursts may be intimately linked with SNe (e.g., GRB980425 and SN 1998bw (Kulkarni et al., 1998); GRB011121 and SN 2001ke (Garnavich et al., 2003); GRB030329 and SN 2003dh (Stanek et al., 2003)), such studies are crucial to understanding GRB environments. To date, radio emission has only ever been detected from core-collapse SNe of Type II and Type Ib/c (for a review of supernova taxonomy, see Turatto (2003)), and not at all from thermonuclear Type Ia SNe (Panagia et al., 2006).

In the local Universe (here defined to extend out to roughly 30 Mpc), approximately 3–6 supernova events are discovered optically each year, of which 1–2 per year are also detected at radio wavelengths. A galaxy like our Milky Way has one of its massive stars explode only about every 100 years, making it very difficult to identify and study the star prior to its death; only once the star has exploded does it become fairly easy to see where our telescopes should have been trained for the previous centuries to study the end-stage of the progenitor stars evolution. Fortunately, nature has provided us with the astrophysical equivalent of recovering an airplane's black box after an explosion; we can piece together vital clues about the star's life in its death. In the years prior to their deaths, most stars shed their outer layers in the form of a significantly enhanced wind. The slow moving winds associated with these very massive stars can shed roughly 10% of the Sun's total mass in just 1000 years. When the star finally dies, the explosion resulting from the supernova moves outward with a speed roughly 1000 times that of the wind. When the blast hits the wind, the electrons get swept up in the blastwave and emit radio emission. As the blastwave moves farther and farther outward, it encounters the wind shed by the star at earlier and earlier epochs. For every year we monitor and study the radio emission from a new supernova, we can discern the history of its mass-loss over a 1,000 year period, and some SNe have emission that persists for decades.

VAST will provide the first unbiased census of core-collapse SNe, by allowing us to match radio detections against optically-discovered SNe. We should also detect new radio SNe that may have gone undetected in the optical or infrared due to significant amounts of dust (Kankare et al., 2008). Every new SN discovery is valuable for tying down the current rate of massive star formation in the Universe and for understanding how and when SNe explode in star-bursting galaxies. Core-collapse SNe "turn on" within days, and reach their peak luminosity at 1.4 GHz as much as one year after explosion, typically $\sim$ 1 mJy at a distance of 50 Mpc (Gal-Yam et al., 2006), making them ideal targets to study with the sensitivity and cadence of VAST. With our planned survey, we would expect to detect $\sim$1 SN per month.

2 Radio light curve characteristics

There have been over 40 radio-detected SNe, with low radio upper limits established for over 120 others (see the compilation at http://rsd-www.nrl.navy.mil/7213/weiler/kwdata/rsnhead.html and Table 1 of Weiler et al. (2002)). Clearly the radio sampling is quite limited compared to the total number of SN events, with around 500 optical discoveries per year, and several thousand SNe in total having been observed with optical telescopes. All of these radio detections are core collapse SNe (Types Ib, Ic, and II). The various sub-types of type SNe II (IIP, IIL, IIn, IIb) comprise $\sim$75% of all radio-detected SNe.

The radio "light curve" of a supernova can be broadly divided into three phases: first, there is a rapid turn-on with a steep spectral index ($\alpha > 2$, so the SN is brightest at the higher frequencies), due to a decrease in the line-of-sight absorption. After some weeks or months have elapsed, the flux reaches a peak, turning over first at the highest frequencies. Eventually, the SN begins to fade steadily, and at the same rate at all frequencies, in the optically-thin phase. As the evolution is most rapid in the early phases, radio light curves are normally plotted on a log–log scale (e.g. SN 1993J: Figure 1). The ionised CSM (free-free absorption; FFA) is the primary source of the initial absorption in young SNe, with synchrotron self-absorption (SSA) playing a role in some specific cases (Chevalier, 1998). Under the simplest of models, the CSM is assumed to have been established by a constant, spherically-uniform mass-loss rate, as a constant velocity wind from a massive progenitor or companion star, resulting in a uniformly declining density with radius (for FFA; Chevalier 1982).

The general properties of supernova radio light curves as outlined above are quite well represented by a modified version of the "minishell" model of Chevalier (1982), and have been successfully parameterised for more than a dozen SNe (see Table 1). Radio synchrotron emission is produced when the SN shock wave ploughs into an unusually dense circumstellar medium (CSM). Following the notation of Weiler et al. (2002) and Sramek & Weiler (2003), we model the multi-frequency evolution as:

$$S(\mathrm{mJy}) = K_1\left(\frac{\nu}{5\ \mathrm{GHz}}\right)^{\alpha}\left(\frac{t-t_0}{1\ \mathrm{day}}\right)^{\beta} e^{-\tau_{\mathrm{ext}}} \times\left(\frac{1-e^{-\tau_{\mathrm{CSM_{clumps}}}}}{\tau_{\mathrm{CSM_{clumps}}}}\right)\left(\frac{1-e^{-\tau_{\mathrm{int}}}}{\tau_{\mathrm{int}}}\right) \qquad (1)$$

with

$$\tau_{\mathrm{ext}} = \tau_{\mathrm{CSM_{homog}}} + \tau_{\mathrm{distant}} \qquad (2)$$

where

$$\tau_{\mathrm{CSM_{homog}}} = K_2\left(\frac{\nu}{5\ \mathrm{GHz}}\right)^{-2.1}\left(\frac{t-t_0}{1\ \mathrm{day}}\right)^{\delta}, \qquad (3)$$

$$\tau_{\mathrm{distant}} = K_4\left(\frac{\nu}{5\ \mathrm{GHz}}\right)^{-2.1}, \qquad (4)$$

and

$$\tau_{\mathrm{CSM_{clumps}}} = K_3\left(\frac{\nu}{5\ \mathrm{GHz}}\right)^{-2.1}\left(\frac{t-t_0}{1\ \mathrm{day}}\right)^{\delta'}, \qquad (5)$$

with the various K terms representing the flux density (K_1), the attenuation by a homogeneous absorbing medium (K_2, K_4), and by a clumpy/filamentary medium (K_3), at a frequency of 5 GHz one day after the explosion date t_0. The $\tau_{\mathrm{CSM_{homog}}}$ and $\tau_{\mathrm{CSM_{clumps}}}$ absorption arises in the circumstellar medium external to the blast wave, while τ_{distant} is a time-independent absorption produced by e.g., a foreground H II region or more distant parts of the CSM unaffected by the shock wave (Figure 2). The spectral index is α; β gives the rate of decline in the optically-thin phase; and δ and δ' describe the time dependence of the optical depths in the local homogeneous, and clumpy/filamentary CSM, respectively (see Weiler et al. (2002) and Sramek & Weiler (2003) for a detailed account of how these parameters are related). The internal absorption τ_{int} can be further broken down into FFA and SSA components (Weiler et al., 2007), but high frequency observations at early times are needed to properly constrain these, which are rarely obtained.

Not all supernovae adhere strictly to this regime, and often those that do not are the ones that offer us the most insight into the nature of the progenitor object. For instance the radio light curve of the Type IIb SN 2001ig (Ryder et al., 2004) showed bumps and dips in flux with a periodicity ∼150 days (Figure 3), suggestive of "sculpting" of the CSM by the action of a binary companion, the existence of which was subsequently confirmed by observations with Gemini (Ryder et al., 2006).

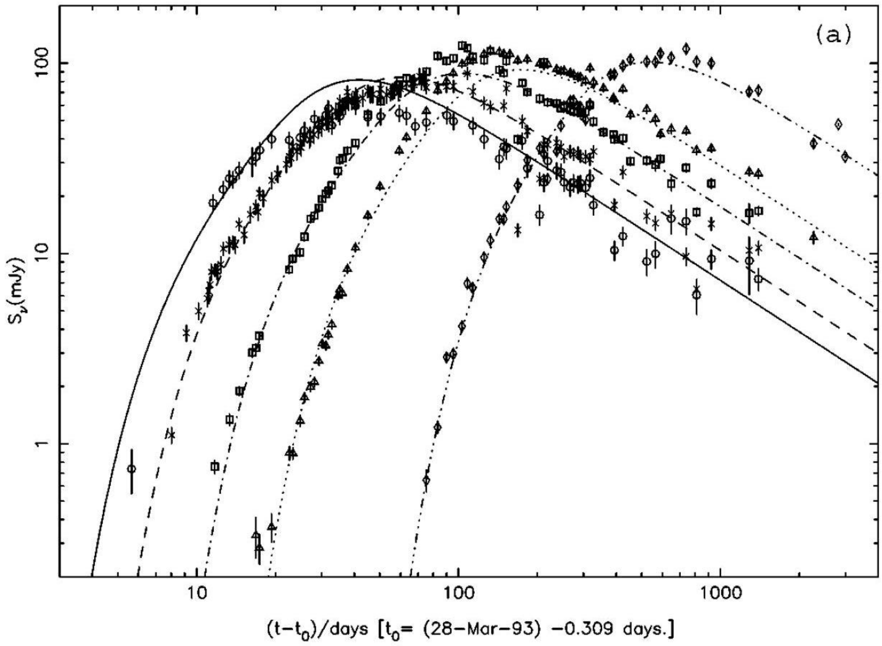

Figure 1: VLA radio fluxes for the Type IIb SN 1993J overlaid with model fits as parameterised by equations 1–5 in Section 2 taken from Weiler et al. (2002). Fluxes and fits are shown for 22.5 GHz (open circles, solid line); 14.9 GHz (stars, dashed line); 8.4 GHz (open squares, dash-dot line); 4.9 GHz (open triangles, dotted line); and 1.5 GHz (open diamonds, dash-triple dot line).

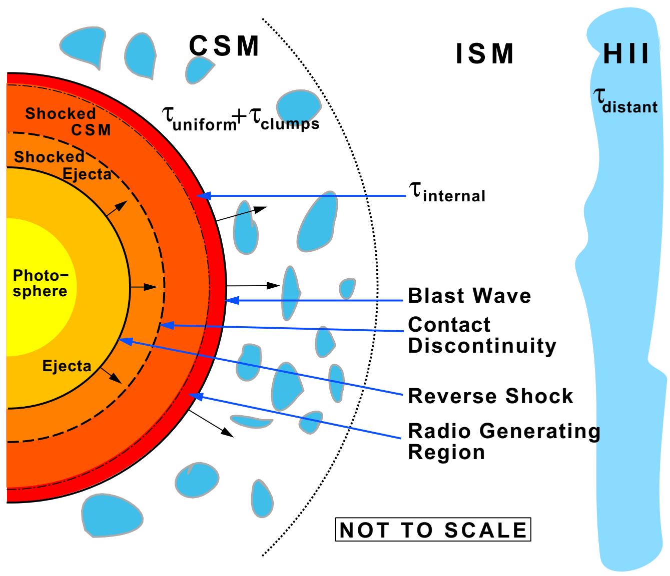

Figure 2: Cartoon image of the SN blastwave interacting with the CSM (Stockdale et al., 2009). The various absorption sources are indicated.

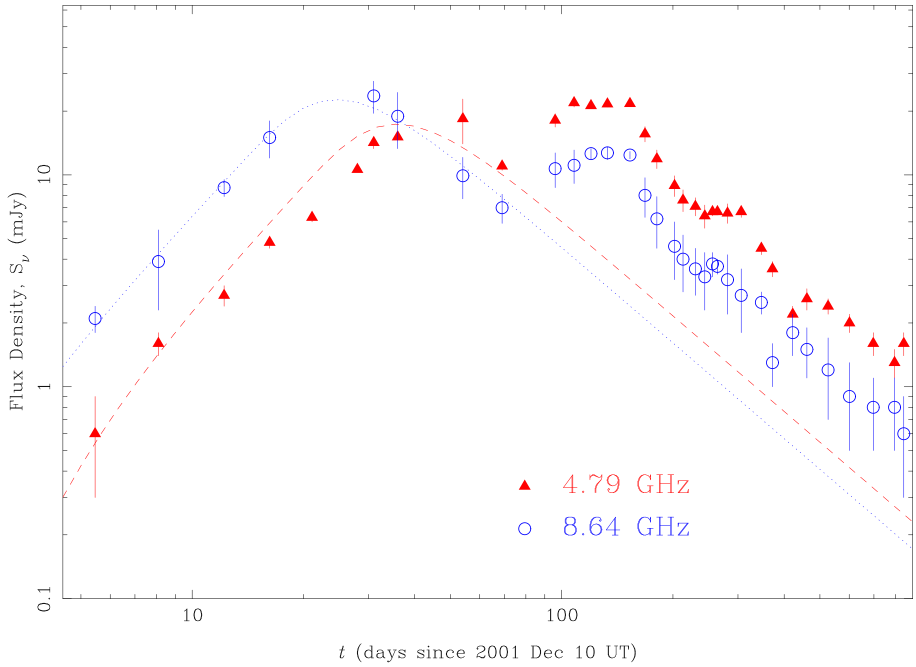

Figure 3: ATCA radio fluxes for SN 2001ig overlaid with model fits to the first 50 days of data. At later times the blastwave probes a CSM which has been modulated by the orbital effect of a binary companion star (Ryder et al., 2004, 2006).

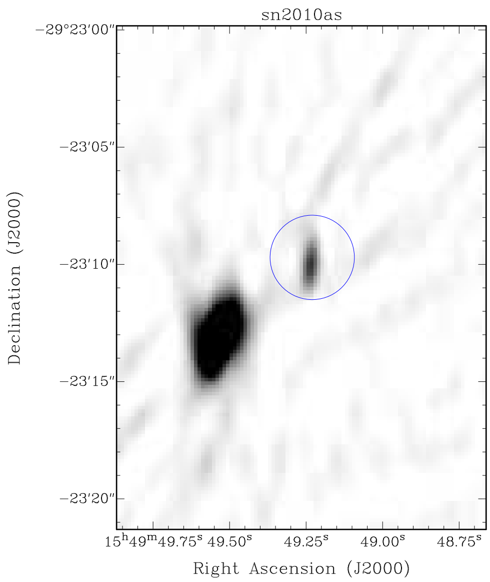

Figure 4: ATCA image of SN 2010as in NGC 6000 at 9 GHz with CABB. The SN is marked by the blue circle, just 5″ away from the starburst nucleus (Ryder et al., 2010).

3 Simulating Supernovae in VAST

Table 1 summarises the best-fit model parameters described above for the 15 core-collapse SNe for which sufficient light curve information is available in the literature. While not a completely representative sample, and no doubt biased somewhat towards the more luminous events, these are indicative of the ranges spanned by these parameters and would permit the simulation of realistic radio light curves for use in ASKAP simulations. The time from explosion to peak brightness at 5 GHz, and the 5 GHz peak luminosity are also included in the Table, although these are set by the other parameters plus the distance to the SN.

Supernovae in general are not seen in isolation, but are usually superimposed on a diffuse, non-thermal background from their host galaxy. They may also appear in close proximity to an AGN or starburst nucleus, e.g. SN 2010as in NGC 6000 (Figure 4). As none of these young SNe will be resolvable with ASKAP, the confusing effect of the diffuse background can be minimised, and separation from any bright nuclear component maximised, by **heavily favouring the longest baselines**. The SNe in Table 1 lie between 0.1 and 6.6 arcminutes from the nuclei of their host galaxies.

Since "hostless" SNe in the local Universe are almost unheard of, one possible way to speed up the search for SN candidates in any catalog of transients or all-sky map would be to limit the search to within a radius of 15 arcminutes of the position of all catalogued galaxies out to 30 Mpc. This would cover all galaxies south of Declination $+30°$ except the LMC, SMC, and Sagittarius Dwarf.

A Fortran example of the algorithms used to generate the light curves in Figures 1 and 3 follows. The array `t(i)` contains $\log_{10}$ of the time in days since explosion, while `modflux(i)` contains $\log_{10}$ of the flux in mJy at time `t(i)`, at frequency `nu`.

```
      program rlc

      implicit none
      real k1,alpha,beta,k2,k3,k4,nu,delta,delta2,t(50),modflux(50),fy
      integer i

      write(6,*)'Enter unabsorbed flux density K_1'
      read(5,*)k1
      write(6,*)'Enter spectral index alpha'
      read(5,*)alpha
      write(6,*)'Enter evolution index beta'
      read(5,*)beta
      write(6,*)'Enter uniform optical depth K_2'
      read(5,*)k2
      write(6,*)'Enter non-uniform optical depth K_3'
      read(5,*)k3
      write(6,*)'Enter thermal optical depth K_4'
      read(5,*)k4
      delta = alpha - beta - 3
      delta2 = 5*delta/3

      nu=1.38
      do 100 i=1,50
         t(i)=0.6+(i*0.07)
         modflux(i)=fy(t(i),nu,delta,delta2,k1,k2,k3,k4,alpha,beta)
 100  continue

      function fy(t,nu,delta,delta2,k1,k2,k3,k4,alpha,beta)
      real tmt0,tau,tau2,t,nu,delta,delta2,k1,k2,k3,alpha,beta
      real tau3,k4

      tmt0=10.0**t
      tau = k2 * ((nu/5.0)**(-2.1)) * (tmt0**delta)
```

```
      tau2 = k3 * ((nu/5.0)**(-2.1)) * (tmt0**delta2)
      tau3 = k4 * ((nu/5.0)**(-2.1))
      fy = k1 * ((nu/5.0)**alpha) * (tmt0**beta) *
     &     (exp(-1.0*(tau+tau3))) * ((1 - (exp(-1.0*tau2)))/tau2)
      fy = alog10(fy)
      return
```

References

Chevalier R. 1982, ApJ, 259, 302

Chevalier R. 1998, ApJ, 499, 810

Gal-Yam, A., Ofek, E. O., Poznanski, D., Levinson, A., Waxman, E., Frail, D. A., Soderberg, A. M., Nakar, E., Li, W., & Filippenko, A. V. 2006, ApJ, 639, 331

Garnavich P. M., et al. 2003, ApJ, 582, 924

Kankare, E., Mattila, S., Ryder, S. D., Perez-Torres, M. A., Alberdi, A., Romero-Canizales, C., Diaz-Santos, T., Väisänen, P., Efstathiou, A., Alonso-Herrero, A., Colina, L., & Kotilainen, J. 2008, ApJ, 689, L97

Kulkarni, S. R., et al. 1998, Nature, 395, 663

Montes, M. J., Van Dyk, S. D., Weiler, K. W., Sramek, R. A., & Panagia, N. 1998, ApJ, 506, 874

Panagia, N., Van Dyk, S. D., Weiler, K. W., Sramek, R. A., Stockdale, C. J., & Murata, K. 2006, ApJ, 646, 369

Ryder, S. D., Covarrubias, R., Amy, S. W., Argo, M., Stockdale C., Van Dyk, S., Immler, S., Weiler, K. W., & Panagia, N. 2010, CBET 2242.

Ryder, S. D., Murrowood, C. E., & Stathakis, R. A. 2006, MNRAS, 369, L32

Ryder, S. D., Sadler, E. M., Subrahmanyan, R., Weiler, K. W., Panagia, N., & Stockdale, C. J. 2004, MNRAS, 349, 1093

Schlegel, E. M., Ryder, S. D., Staveley-Smith, L., Petre, R., Colbert, E. M., & Dopita, M. A. 1999, AJ, 118, 2689

Sramek, R. A., & Weiler, K. W. 2003, in Weiler K. W., ed., Supernovae and Gamma-Ray Bursters. Springer-Verlag, Berlin, p. 145

Stanek, K. Z., et al. 2003, ApJ, 591, L17

Stockdale, C., Weiler, K., Panagia, N., Sramek, R., van Dyk, S., Immler, S., Pooley, D., Marcaide, J., Ryder, S., Kelley, M., & Williams, C. 2009. White Paper submitted to the Astro2010 Stars and Stellar Evolution (SSE) panel (arXiv:0902.4059)

Stockdale, C. J., Weiler, K. W., Van Dyk, S. D., Montes, M. J., Panagia, N., Sramek, R., Perez-Torres, M. A., & Marcaide, J. M. 2003, ApJ, 592, 900

Turatto, M. 2003, in Weiler K. W., ed., Supernovae and Gamma-Ray Bursters. Springer-Verlag, Berlin, p. 21

Weiler, K. W., Panagia, N., Montes, M., & Sramek, R. A. 2002, ARA&A, 40, 387

Weiler, K. W., Sramek, R. A., Panagia, N., van der Hulst, J. M., & Salvati, M. 1986, ApJ, 301, 790

Weiler, K. W., Williams, C. L., Panagia, N., Stockdale, C. J., Kelley, M. T., Sramek R. A., Van Dyk, S. D., & Marcaide, J. M. 2007, ApJ, 671, 1959

Table 1: Model fitting parameters for 15 core-collapse supernovae with well-sampled radio light curves. Reference “RSN” corresponds to the compilation by K. W. Weiler at http://rsd-www.nrl.navy.mil/7213/weiler/sne-home.html. The time from explosion until peak brightness at 5 GHz (T_{peak}), and the 5 GHz luminosity at that time (L_{peak}) are also included.

SN	Type	D (Mpc)	K_1 (mJy)	K_2	K_3	K_4	α	β	δ	δ'	T_{peak} (days)	L_{peak} (erg s^{-1} Hz^{-1})	Ref
1983N	Ib	4.6	3.3×10^3	3.0×10^2	0	0	−1.08	−1.55	−2.53	0	12	1.0×10^{27}	RSN
1984L	Ib	18.8	2.5×10^2	4.8×10^1	0	0	−1.14	−1.50	−2.64	0	6	4.9×10^{27}	RSN
1990B	Ic	18.3	1.9×10^2	1.3×10^4	0	0	−1.08	−1.26	−2.82	0	40	5.2×10^{26}	RSN
1994I	Ic	7.8	8.7×10^3	3.4×10^1	2.5×10^4	0	−1.16	−1.57	−1.64	−2.70	...	...	Weiler et al. (2002)
1993J	IIb	3.63	4.9×10^3	1.7×10^2	4.3×10^5	0	−0.82	−0.73	−1.42	−2.84	133	1.5×10^{27}	Weiler et al. (2007)
2001gd	IIb	21.6	1.49×10^3	3.25×10^6	1.05×10^3	0	−1.38	−0.96	−3.0	−1.27	173	2.9×10^{27}	Stockdale et al. (2003)
2001ig	IIb	11.5	2.71×10^4	1.38×10^3	1.47×10^5	0	−1.06	−1.50	−2.56	−2.69	74	3.5×10^{27}	Ryder et al. (2004)
1970G	IIL	7.2	1.8×10^6	1.8×10^7	0	0	−0.55	−1.87	−3.00	0	...	...	RSN
1979C	IIL	15.9	1.7×10^3	3.4×10^7	0	0	−0.75	−0.80	0	0	556	2.2×10^{27}	RSN
1980K	IIL	6.9	1.2×10^2	1.4×10^5	0	0	−0.60	−0.73	−2.68	0	130	1.1×10^{26}	Montes et al. (1998)
1981K	II	7.5	7.6×10^1	1.0×10^4	0	0	−0.74	−0.70	−3.04	0	34	3.5×10^{26}	RSN
1982aa	II?	70	5.3×10^4	3.5×10^7	0	0	−0.73	−1.22	−2.96	0	476	1.1×10^{29}	RSN
1978K	IIn	4.0	4.0×10^8	4.5×10^5	1.5×10^{12}	9×10^{-3}	−0.77	−1.55	−2.22	−3.7	970	1.2×10^{28}	Schlegel et al. (1999)
1986J	IIn	7.5	7.6×10^1	1.0×10^4	0	0	−0.74	−0.70	−3.04	0	34	3.5×10^{26}	RSN
1988Z	IIn	70	1.2×10^4	0	3.2×10^8	0	−0.72	−1.22	0	0	911	1.1×10^{28}	RSN